Inorganic Chemistry
Cite This: Inorg. Chem. 2019, 58, 8486−8493
Article
pubs.acs.org/IC

Lighting the Flavin Decorated Ruthenium(II) Polyimine Complexes: A Theoretical Investigation

Huimin Guo,*[,†] Can Dang,[†] Jianzhang Zhao,*[,†] and Bernhard Dick[‡]

[†]State Key Laboratory of Fine Chemicals, School of Chemistry, Dalian University of Technology, Dalian, 116024, P. R. China
[‡]Institut für Physikalische und Theoretische Chemie, Universität Regensburg, Regensburg, 93053, Germany

Supporting Information

ABSTRACT: The emission properties of a series of flavin (FL) decorated Ru (II) polyimine complexes were investigated by extensive time-dependent (TD) density functional theory (DFT) and DFT based calculations. We attributed the moderate emission properties of FL decorated Ru(II) polyimine complex (Ru-1), such as triplet lifetime and luminescence quantum yield, to the dominant fast nonradiative decay due to the small adiabatic energy gap between the ground state and the lowest lying triplet state (ΔE_{ad}) and the slow radiative decay owing to the ligand localized triplet (^{3}IL) nature of the emissive state. Electron withdrawing groups such as F and Cl were attached to the FL moiety of Ru-1 to alter ΔE_{ad}. Both the radiative and nonradiative decay rates were found to be sensitive to ΔE_{ad} and may result in a drastic change of the photophysical properties of the Ru(II) complexes. Specifically, substitution with F leads to an increase in the ΔE_{ad} from 1.85 to 1.93 eV, resulting in a nearly doubled phosphorescent quantum yield and triplet lifetime with respect to Ru-1. These findings are vital for the rational design of phosphorescent transition metal complexes.

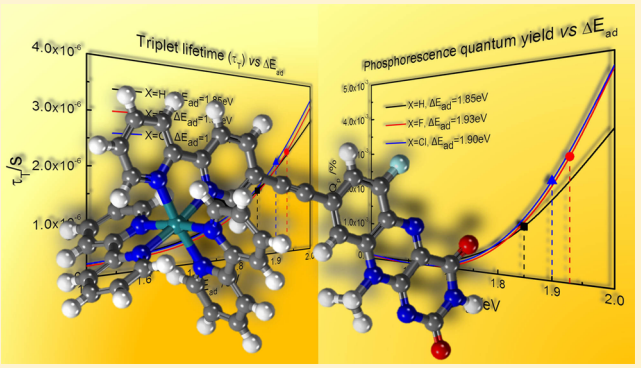

INTRODUCTION

Transition metal complexes, especially complexes of Pt(II), Ir(III), Ru(II), etc., have drawn considerable attention for their outstanding photophysical properties, which enable their applications as photosensitizers in photocatalysis,[1−5] phosphorescent imaging and molecular sensing,[6−10] photodynamic therapy,[11−13] triplet−triplet annihilation upconversion,[14,15] etc.

When photoexcited at a suitable wavelength, the molecules of a transition metal complex go first from the ground state (S_0) to the dipole-allowed excited states (S_n). The allowed S_0 to singlet metal−ligand charge transfer state (^{1}MLCT) transition results in a generally weak absorption band as compared with the organic dyes.[16−19] The excited molecules evolve mainly from the low-lying excited states (S_n) via radiative or nonradiative decay (via vibronic coupling) to S_0.[20] The efficient spin−orbital coupling (SOC) of transition metal centers may also facilitate the excited sensitizer to undergo intersystem crossing (ISC) to reach triplet states with lower energy, and the observed emission of a transition metal complex can be from the low-lying triplet excited states (T_n) competing with vibronic nonradiative decay.[20] Obviously, strong absorption in the visible light region and a triplet emissive state with a longer lifetime are always desired to achieve both energy efficient excitation of photosensitizers and a higher concentration of excited photosensitizer for efficient electron/energy transfer.[6,21−23] Slow radiative and nonradiative decay are expected for a prolonged triplet excited state lifetime and are commonly realized by tuning the relative energy level of the low-lying triplet excited state with the desired ligand localized triplet (^{3}IL) nature.[21−24] Directly attaching a chromophore to the metal center does not guarantee the formation of the desired ^{3}IL state with a prolonged lifetime as the requested energy and spatial requirements may not be satisfied.[25,26] These make the photosensitizer design not straightforward.[21−24,27]

Recently, density functional theory (DFT)/time-dependent (TD)-DFT based calculations have been important tools to understand or predict photophysical properties of transition metal complexes.[28−35] On the basis of the fundamental first-order perturbation rate theory, the radiative decay rate is directly proportional to the SOC between the triplet emissive states and the perturbing states (including S_0) with different multiplicities (H_{SO}), and the electronic transition dipole moment between the involved electronic states with the same multiplicity, and is proportional to the energy gap between the involved singlet and triplet states.[36] The nonradiative decay rates between the triplet and singlet states can be predicted with H_{SO}, energy gaps, and vibronic coupling.[37−40] Combining these theoretical predicted parameters with ligand design and experimental investigations may help to understand the correlation between the ligand structure

Received: March 12, 2019
Published: June 7, 2019

DOI: 10.1021/acs.inorgchem.9b00713
Inorg. Chem. 2019, 58, 8486−8493

and radiative properties for a rationalized application-oriented design of transition metal complexes.[41]

Owing to its superior photophysical properties, advantageous electrochemical behavior, and chemical robustness, Ru(II) bipyridine complex ($[Ru(bpy)_3]^{2+}$, bpy = 2,2′-bipyridine, Ru-0) and Ru(II) complexes derived from Ru-0 have been widely used in lighting devices,[42] photodynamic therapy,[43] solar cells,[44] sensors,[45] photocatalysis,[46,47] etc. Recently, we connected flavin (FL) to a bipyridyl ligand and synthesized an FL decorated Ru(II) bipyridine complex (Ru-1). In this way, we enhanced the absorption in the visible light region with respect to Ru-0 and observed phosphorescence emission from the ^{3}IL state originated from the FL moiety of Ru-1. However, the T_1 lifetime and triplet quantum yield of Ru-1 are only moderate.[26] This makes it highly desired to find the dominant factors for the radiative or nonradiative rates of Ru-1 theoretically. In this work, we investigated the photophysical properties of Ru-1-Cl and Ru-1-F and compared them with those of Ru-1 and the model compound Ru-0 to understand the factors that govern the radiative and nonradiative decay processes. We expect the findings may help to guide the design of photosensitizers of this type.

THEORETICAL METHODS

The compounds investigated are shown in Figure 1, including flavin (FL), FL decorated bipyridyl ligand (L-1), FL decorated Ru(II) bipyridine complex and derivatives (Ru-1-X), and Ru(II) bipyridine complex (Ru-0). The recent experimental research showed that only the ground state (S_0), the first singlet excited state (S_1), and the first triplet excited state (T_1) of these compounds are involved in the photophysical processes of these compounds under radiation at 430 nm.[26] The ground state structure (S_0) was optimized with 6-31G(d)[48−50] and LanL2dz basis sets with B3LYP functional,[51,52] while those of excited states (both T_1 and S_1) were fully relaxed within the TD-DFT method at the same level of theory. The impact of solvent was handled with the polarizable continuum model.[53−55] All these structures were confirmed with frequency analysis, and these calculations were done with Gaussian 09.[56−58] The SOC matrix elements were calculated with the default scale charge for Ru using the one-electron Breit-Pauli operator, and together the $T_1 \rightarrow S_0$ electronic transition dipole moments[59−61] were calculated with Dalton 2016 with the aforementioned DFT/TD-DFT approach.[62−64] The theoretical estimates for the radiative and nonradiative decay rate constants of the $T_1 \rightarrow S_0$ transition were obtained with the methodology developed by Shuai and co-workers as implemented in MOMAP.[36,40,65−67] Briefly, the rate constants were obtained by a Franck−Condon weighted average over all vibrational modes in the initial and final electronic states, which includes a Boltzmann distribution for the thermal population of the initial vibrational states. The multidimensional Franck−Condon integrals were evaluated by Fourier transform of the thermal vibrational correlation function. The result is the temperature-dependent and vibrationally resolved phosphorescence spectrum, which, after integration, yields the radiative rate constant. These setups were found to be efficient to study the emission properties of Ir(III) complexes and photophysics of some organic dyes.[29,41]

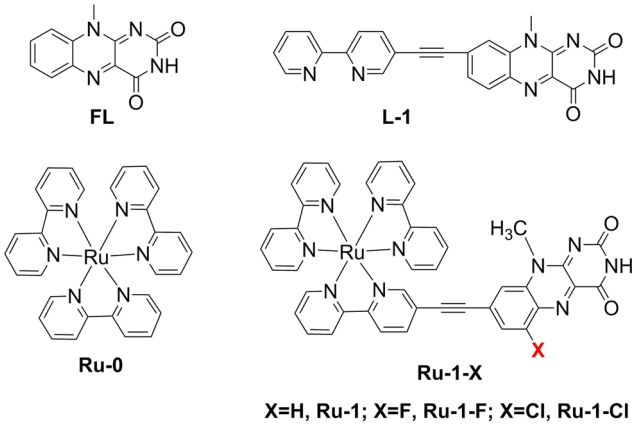

Figure 1. Structures of compounds, including FL, L-1, Ru-0, and Ru-1-X (X = F and Cl). Ru-0, Ru-1-F, and Ru-1-Cl are in their +2 charged state.

RESULTS AND DISCUSSION

Experimental investigation already showed that the phosphorescent emission of these compounds were from their T_1 under radiation at 430 nm.[26] We first investigated the electronic structure of the T_1 of Ru-0, Ru-1, FL, and L-1 to understand the origin of the emission (Figure 2). In accordance with the lowest energy electronic transition for the excitation of Ru-0 that is from the Ru-d states to the π^* state of bipyridine ligand (Table S1 and Figure S1), the spin density is distributed on Ru(II) center and one of the bipyridine ligand (Figure 2a), providing direct evidence for the ^{3}MLCT nature of T_1 of Ru-0 (Figure 1). The T_1 spin density spatial distribution of Ru-0 and Ru-1 are quite different. In Ru-1, the T_1 spin density is distributed within the L-1, mainly localized on the FL moiety (Figure 2b) and decreases gradually within the bipyridine ligand with negligible contribution from the Ru-d states, showing the dominant intraligand charge transfer (^{3}IL) nature of the Ru-1 T_1 state. Further, the T_1 state in Ru-0 is extended to include the conjugated framework of FL in Ru-1. With these, we can expect that the emission spectra of Ru-0 and Ru-1 would be quite different as their T_1 are of different origins. This is supported by the experimentally observed emission at 595 and 643 nm for Ru-0 and Ru-1, respectively, and the calculated $S_0 \rightarrow T_1$ vertical excitation of 648 nm for Ru-1 (Table S2 and Figure S2). A close examination of Figure 2b−d shows that the T_1 spin density of Ru-1, FL, and L-1 are similar not only for the spatial distribution but also for the phase of

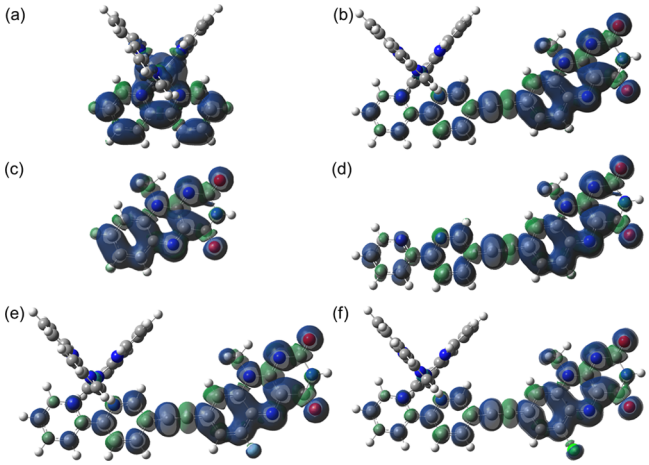

Figure 2. Isosurface plots of TDDFT calculated T_1 spin density of Ru-0 (a), Ru-1 (b), FL (c), L-1 (d), Ru-1-F (e), and Ru-1-Cl (f). (isovalue = 0.0004 au, the Ru, C, O, N, H, F, Cl, etc. are in cyan, gray, red, blue, white, light green, and bright green, respectively.) The detailed values of spin density projected to each atom can be found in Figures S3−S8 and Tables S3−S8.

DOI: 10.1021/acs.inorgchem.9b00713
Inorg. Chem. 2019, 58, 8486−8493

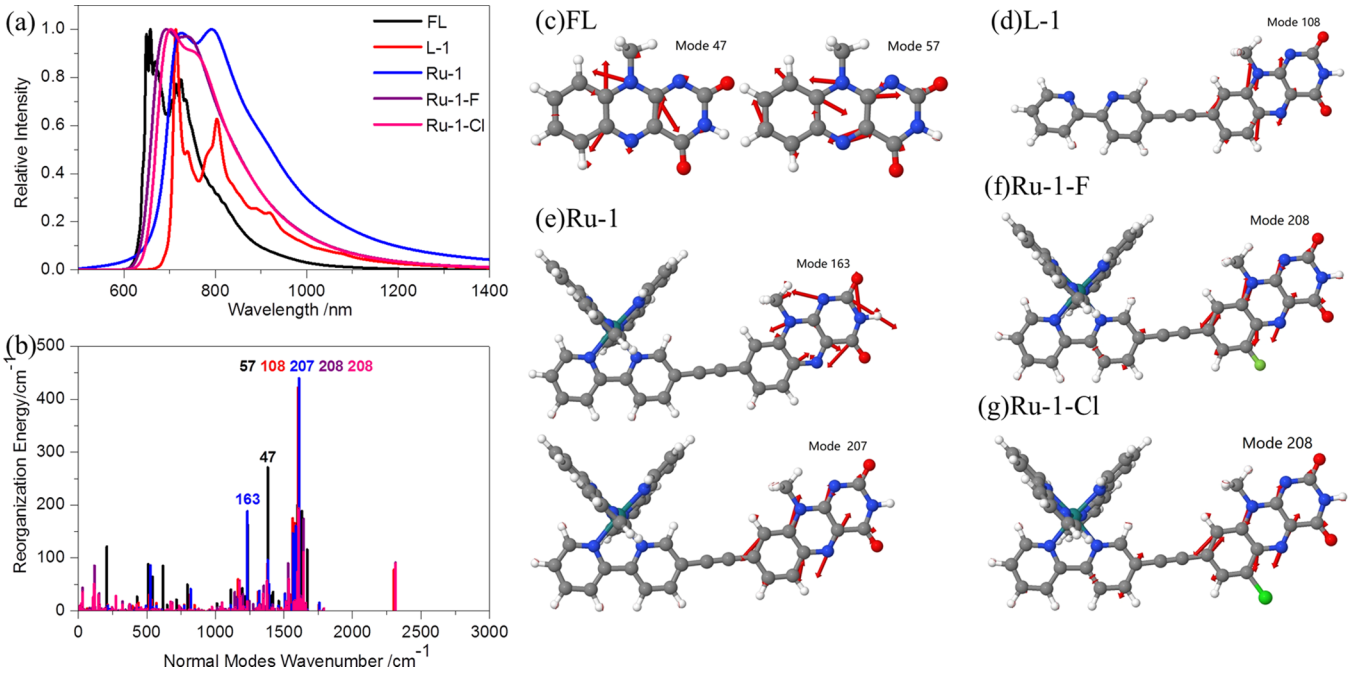

Figure 3. Simulated phosphorescence spectra of FL, L-1, Ru-1, Ru-1-F, and Ru-1-Cl (a), the projection of reorganization energy into normal modes on corresponding S_0 potential surface (b) and the vectorized representation of atomic displacement for the corresponding vibration modes of FL (c), L-1 (d), Ru-1 (e), Ru-1-F (f), and Ru-1-Cl (g). The spectra were simulated at 298 K.

Table 1. Calculated Photophysical Properties of Ru Complexes at 298 K

298 K	Ru-0	Ru-1	Ru-1-F	Ru-1-Cl
k_r/s^{-1}[a]	1.76×10^5	8.11	11.78	10.64
k_{nr}/s^{-1}[b]	1.11×10^5	6.82×10^5	4.22×10^5	4.72×10^5
$Q_P/\%$[c]	61.30	1.19×10^{-3}	2.79×10^{-3}	2.26×10^{-3}
μ/Debye[d]	0.4132	0.003934	0.004346	0.004191
H_{SO}/cm^{-1}[e]	5.33	1.51	1.64	1.61
E_{reorg}/cm^{-1}[f]	2188.24	1674.89	1481.58	1432.92

[a]Radiative decay rate constant. [b]Nonradiative decay rate constant. [c]Theoretical phosphorescent emission quantum yield in percentage, calculated as $k_r/(k_r + k_{nr}) \times 100\%$. We only considered the S_0, S_1, and T_1 for Ru-0, and the value was overestimated as compared with the experimental values.[71] [d]The electric transition dipole moment between the involved electronic states with the different multiplicities calculated quadratic response function with Dalton.[36,72] Please consult ref 36 for the details on calculation of this electric transition dipole moment. [e]The averaged spin−orbit coupling matrix elements between the emitting states and the perturbing states with different multiplicity,[36,73,74] calculated as $\text{ave} = \sqrt{(|\langle S_0|\hat{H}^{SO}|T_{1,x}\rangle|^2 + |\langle S_0|\hat{H}^{SO}|T_{1,y}\rangle|^2 + |\langle S_0|\hat{H}^{SO}|T_{1,z}\rangle|^2)/3}$. [f]Reorganization energy, calculated as the difference in energy of the T_1 and S_0 structures on the S_0 potential energy surface.

the spin wave function, implying that Ru-1 would exhibit phosphorescence emission similar to those of FL and L-1.

The simulated vibrationally resolved phosphorescent spectra of FL, L-1, and Ru-1 were compared in Figure 3 to highlight the origin of emission of Ru-1 T_1 state. The emission maximum (λ_{em}) of the simulated phosphorescent spectra of Ru-1 and L-1 is at ∼660 nm (Figure 3a), in reasonable agreement with the experimental λ_{em} of 643 nm and the calculated $S_0 \rightarrow T_1$ vertical excitation at 648 nm (Table S2).[26] The emission spectra of L-1 and Ru-1 are similar and are all red-shifted by ∼50 nm with respect to that of FL. The emission wavelength is determined by adiabatic S_0-T_1 band gap (ΔE_{ad}) and the vibrational reorganization after electronic transition along the S_0 potential energy surface (reorganization energy, E_{reorg}). The calculated ΔE_{ad} values of FL, L-1, and Ru-1 are 2.00, 1.85, and 1.85 eV, respectively, and the difference is because FL extends the conjugation in L-1 and lowers the energy difference of frontier states that determines ΔE_{ad}. The calculated E_{reorg} values of FL, L-1, and Ru-1 are 0.21, 0.20, and 0.21 eV, respectively. The small E_{reorg} values can thus be attributed to the renowned small reorganization of FL derivatives and the similarity of the bonding within the FL moiety in L-1 and Ru-1. We then projected the T_1 structure to ground state normal modes to correlate the energy transition with the atomic structures (Figure 3b). The E_{reorg} of L-1 (Figure 3d) and Ru-1 (Figure 3e) was found to be contributed mainly by the same groups of normal modes on corresponding S_0 potential energy surface (Figure 3b). We further analyzed the atomic motions related to these normal modes and found that these normal modes can be assigned to the vibration of C and N atoms within the FL moiety (Figure 3c−e). The above findings strengthen our proposal on the important role of the extended conjugation in L-1 to the redshift and the radiative properties of Ru-1. As the impact of temperature and solvent on the emission spectra was already included during the calculation, we propose that the broadening of the emission

DOI: 10.1021/acs.inorgchem.9b00713
Inorg. Chem. 2019, 58, 8486−8493

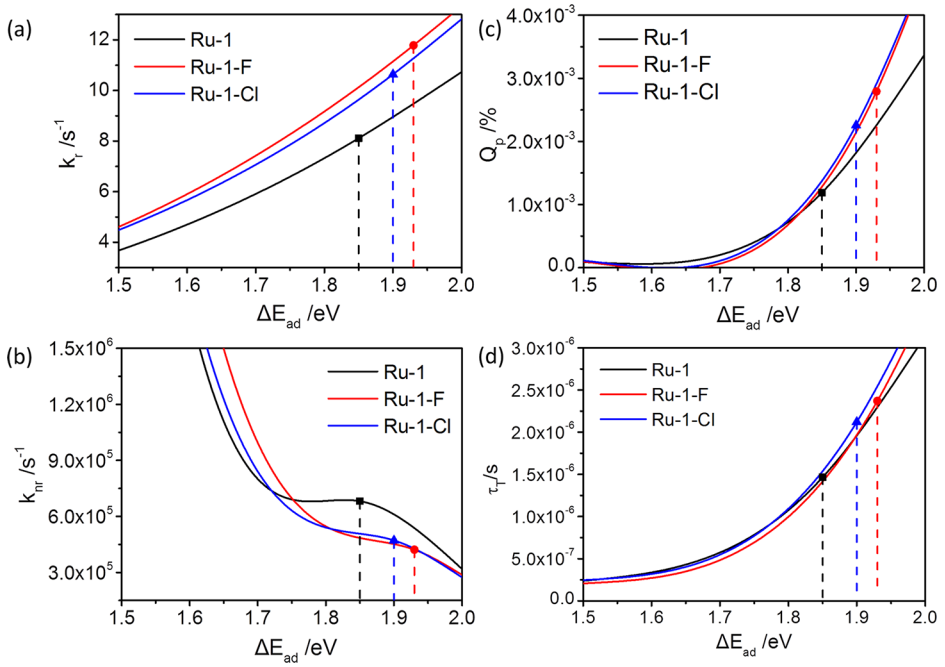

Figure 4. Variation of k_r (a), k_{nr} (b), Q_p (c), and τ_T (d) of Ru complexes with ΔE_{ad}. (The curves were obtained using properties of the corresponding complex by varying only ΔE_{ad}. For clearance, only the points corresponding to ΔE_{ad} of each complex was marked on the corresponding curve. k_r was the integration of the calculated phosphorescence emission spectra (Figure 3a).[36] Though it is currently hard to conclude, k_r may be related to the cubic of ΔE_{ad}.[71] Q_P was calculated as the ratio of radiative decay rate constant and the sum of radiative and nonradiative decay rate constant.)

spectrum of Ru-1 with respect to that of L-1 is due to the coupling of the ground state normal modes of L-1 with those of the Ru(II) center and the bipyridyl ligands.

The luminescence quantum yields of these Ru(II) complex depend on the radiative and nonradiative decay rates from the triplet emissive states. We compared the calculated theoretical photoluminescence properties of Ru complexes in Table 1. The calculated results compare well with the reported experimental investigations of Ru-0 and Ru-1 in the order of magnitude.[26] The calculations were performed based on the fundamental first-order perturbation rate theory.[36] The radiative decay rate constants were calculated as the integration of the emission spectrum. The emission spectra of transition metal complexes are often evaluated at different temperatures in experiments. Low temperature emission spectra, commonly containing sharp peaks corresponding to vibrationally resolved fine-structure features, are widely used to investigate the electronic transitions and electron−phonon interaction. These fine-structure features correspond to the transition from the vibration states of triplet excited state to the vibration states of ground state and the coupling with the ground state normal modes. However, these features are generally not observable in the spectra obtained at elevated temperatures (e.g., room temperature) which contain merely broadened peaks. We calculated the vibrationally resolved emission spectra of Ru-1 at 0 K and found that these fine structures correlate well with the calculated Huang−Rhys factors that are commonly used to characterize vibronic coupling.[26] With thermal vibration correlation function, the emission spectra of Ru-1 at 298 K can be finely reproduced.[68−70] Though the emission spectra vary with temperatures, the calculated the radiative decay rates constants do not vary significantly, and the values at 77, 196, and 298 K are 9.27, 8.65, and 8.11 s^{-1}, respectively. Similar results were reported on room temperature phosphorescent emission Ir(III) complexes.[41] It should be noted that the finding may not hold for those transition metal complexes that the phosphorescent emission processes vary significantly with temperature.

As the scaled charge of transition metal atoms for spin−orbital integral is always 10^3 fold more significant than those of the main group elements, they contribute dominantly to the H_{SO} in transition metal complexes. Therefore, a decrease of the contribution of the transition metal d states to the electronic transition of T_1 may dramatically alter H_{SO} and leading to a drastic change of the transition dipole moment.[41] For Ru-0, T_1 is of MLCT character (Figures 2 and S1), the $S_0 \rightarrow T_1$ coupling is strong according to the symmetry selection rule, and the calculated H_{SO} is 5.33 cm^{-1}. In contrast, the T_1 of Ru-1 is of IL nature and the contribution of the Ru-d orbital for the $S_0 \rightarrow T_1$ transitions is only about 5%, so the calculated H_{SO} is only 1.85 cm^{-1} (Figures 2 and S2). This leads to a significant decrease of the μ of Ru-1 to 0.0039 D, while this value is 0.41 D for Ru-0 where the $S_0 \rightarrow T_1$ transition is typical MLCT with a contribution of Ru-d typically large than 70%. This partially explains the dramatically decrease of the radiative decay rate constants from 1.76×10^5 (Ru-0) to 8.11 s^{-1} (Ru-1) Tables 1 and S1 and S2).

The radiative decay rate is proportional to the adiabatic energy gaps between the involved singlet and triplet states.[36] According to the experiment report on photophysical properties of Ru-1, we have only T_1 and S_0 during the photophysical processes, and their adiabatic energy gap is the ΔE_{ad}.[26] As aforementioned, the introduction of the FL moiety also leads to decreased ΔE_{ad}, from 2.30 eV for Ru-0 to 1.85 eV for Ru-1. We went back to investigate the potential impact of ΔE_{ad} on the photophysical properties of Ru-1. It is not straightforward to alter ΔE_{ad} of a transition metal complex. The introduction of functional groups or extension the conjugation within the

DOI: 10.1021/acs.inorgchem.9b00713
Inorg. Chem. 2019, 58, 8486−8493

organic chromophore may alter ΔE_{ad}. At the same time, the new functional groups and the extended π system may also participate in the conjugation and the bonding within the complex. This may lead to unexpected alternation of H_{so} and μ, which are also vital for the radiative decay. Furthermore, the functional groups may also introduce different energy consumption paths, altering the E_{reorg} and resulting in an unpredictable change of the emission spectra. Inspired by the recent work of Peng and co-workers that the introduction of strong electron withdrawing groups such as F and Cl may alter ΔE_{ad} in a controlled way in Ir(III) complex,[41] we considered F and Cl substituted Ru-1 (Ru-1-F and Ru-1-Cl in Figure 1) and investigated their absorption and emission properties (Tables 1, S9 and S10 and Figures 2, 3, S9 and S10). In short, the electronic transitions of IL character (Figure S9 and S10) that correspond to the absorption of Ru-1-F and Ru-1-Cl appear at 450 and 454 nm, respectively (Tables S9 and S10). According to the isosurface plots of T_1 spin density which are localized only on the substituted L-1 ligands, the T_1 of both Ru-1-F and Ru-1-Cl are of ^{3}IL character (Figure 2f,g, in the right panel). The predicted phosphorescence emission of Ru-1-F and Ru-1-Cl appear at ~640 and ~650 nm, respectively, similar to that of Ru-1 at ~650 nm (Figure 3a), while the identified normal modes on the S_0 potential energy surface that contributed most to the E_{reorg} for Ru-1 derivatives are exactly the same as those for Ru-1 localized within the substituted FL moieties (Figures 3b,f,g). The calculated ΔE_{ad}'s are 1.93 and 1.90 eV for Ru-1-F and Ru-1-Cl, respectively, while the H_{SO}'s are 1.64 and 1.61 cm^{-1}, respectively, and the calculated values of μ are 0.0043 and 0.0042 D, respectively (Table 1). According to the similarities in the calculated values and presented physical pictures for the absorption and emission, we concluded that the electronic structure of Ru-1 framework is preserved to a largest extent in Ru-1-F and Ru-1-Cl. As the calculated μ and H_{SO} for Ru-1-F and Ru-1-Cl are similar to those of Ru-1, while ΔE_{ad}'s vary from 1.85 eV for Ru-1 to 1.93 eV for Ru-1-F, the difference in the calculated radiative decay rate (from 8.11 s^{-1} for Ru-1 to 11.78 s^{-1} for Ru-1-F, Table 1) can be partially attributed to the variation of ΔE_{ad}. The variation of radiative decay rate with respect to ΔE_{ad} was plotted to further verify our proposal on the impact of ΔE_{ad}'s (Figure 4a). Because of the similarity in electronic structure, the curves for the three complexes even overlap in Figure 4. For all three cases, the nonradiative decay rate constants of all three Ru complexes descend slowly with the increase of ΔE_{ad}. However, the radiative decay is promoted by ~50% in Ru-1-F with respect to Ru-1 (Table 1). In this sense, the slow radiative decay of Ru-1 is due to the IL nature of T_1 making the Ru d orbital not effective to contribute to the radiative decay in terms of small μ for the electronic transitions, while the ΔE_{ad} also plays a role.

Nonradiative decay (discussed with calculated the rate constants, as k_{nr}) is always competing with the radiative decay (discussed with calculated the rate constants, as k_r) for excited complexes. For Ru-0, the k_r is comparable with k_{nr}, making the phosphorescent emission quantum yield (Q_P) as high as ~60% (Table 1). As modulated by the IL nature of low-lying excited states (T_1 and S_1) of Ru-1 and substituted derivatives, the k_r decreases significantly, while the k_{nr} remains at the same scale as that of Ru-0 and becomes the dominant decay path, leading to a dramatically decreased Q_P with respect to Ru-0 (Table 1). This makes it also significant to highlight the controlling factors for the nonradiative decay process. The k_{nr} between the T_1 and S_0 depends on the H_{SO}, ΔE_{ad}, etc.[36−40] The H_{SO} values of Ru-1, Ru-1-F, and Ru-1-Cl (of IL character) are smaller than that of Ru-0 (of MLCT character), but they are at the same order of magnitude and their contribution to k_{nr} is expected to be similar. The E_{reorg} of Ru-0 is 0.27 eV, while that of Ru-1 is only 0.21 eV due to the renowned low E_{reorg} of FL derivatives. The E_{reorg} varies only slightly and the contribution to k_{nr} of Ru-1 and its derivatives may not differ significantly. The ΔE_{ad}'s are enhanced to 1.93 and 1.90 eV in Ru-1-F and Ru-1-Cl, respectively, and are thus attributed to impact k_{nr} significantly. To backup this proposal, the variation of k_{nr} with respect to ΔE_{ad} is plotted for Ru-1, Ru-1-F, and Ru-1-Cl (Figure 4b). Because of nearly the same contribution from H_{SO} and E_{reorg}, the k_{nr} curves for these complexes overlap after ΔE_{ad} becomes larger than 1.00 eV. As the ΔE_{ad}'s are significant compared to E_{reorg}'s in Ru-1, Ru-1-F, and Ru-1-Cl, the k_{nr} of these three complexes decrease proportionally with the increase of ΔE_{ad}. Specifically, the increase of ΔE_{ad} from 1.85 eV in Ru-1 to 1.93 eV in Ru-1-F would lead to ~40% decrease of the k_{nr} from 6.82 $\times 10^5$ to 4.22 $\times 10^5$ s^{-1}. This again confirms the dominant contribution of ΔE_{ad} to the outstanding nonradiative decay rate of Ru-1.

Phosphorescence quantum yield (Q_P) and triplet lifetime (τ_T) are two commonly used factors to describe the photophysical properties of a photosensitizer or a luminance material. With the calculated k_r and k_{nr}, the Q_P and τ_T of the three FL decorated Ru(II) bipyridine complexes are also plotted in Figure 4c,d. As nonradiative decay is the main path for the decay of triplet Ru(II) complexes, both k_{nr} and $6Q_P$ are sensitive to and change nearly linear proportionally with ΔE_{ad}. Specifically, a 0.08 eV increase of ΔE_{ad} from Ru-1 leads to nearly doubled Q_P and τ_T for Ru-1-F at 298 K.

CONCLUSIONS

We studied the photophysical properties of a series of FL decorated Ru (II) polyimine complexes by extensive TD/DFT based calculations. We attributed the short triplet lifetime and low luminance quantum yield of Ru-1 with respect to Ru-0 to the fast nonradiative decay due to the small ΔE_{ad} and the slow radiative decay owning to the ^{3}IL nature of the emissive state. We attached electron withdrawing groups such as F and Cl into the FL moiety of Ru-1 and increased ΔE_{ad}. We showed that the nonradiative decay is a dominant decay process, and the decay rates are sensitive to ΔE_{ad} of these complexes. Specifically, substitution with F leads the ΔE_{ad} to increase from 1.85 to 1.93 eV, resulting in nearly doubled phosphorescence quantum yield and triplet lifetime with respect to Ru-1. With these findings, we proposed that FL decorated Ru(II) bipyridine complexes should be redesigned in different ways for application as photosensitizers, molecular sensors, or luminance materials. Slowed k_r and k_{nr} and prolonged τ_T are desired to maintain a higher concentration of the transition metal complexes in triplet excited states for photosensitizer applications, and this can be realized by maintaining an accessible T_1 of IL nature with a large ΔE_{ad}. Fast k_r and slowed k_{nr} are expected to facilitate a transition metal complex with outstanding emission properties for molecular sensing and luminance applications. These require the lowest lying excited states (S_1 and T_1) of partial MLCT character and a significant ΔE_{ad}. These findings may help to rationalize the application-oriented design of transition metal complexes for photosensitizer applications.

DOI: 10.1021/acs.inorgchem.9b00713
Inorg. Chem. 2019, 58, 8486−8493

■ ASSOCIATED CONTENT

Supporting Information

. The Supporting Information is available free of charge on the ACS Publications website at DOI: 10.1021/acs.inorgchem.9b00713.

Electronic transitions contributed to the excitation of Ru-1, FL, L-1, Ru-1-F, and Ru-1-Cl contour plots of wave functions of molecular states involved in these transitions, optimized T_1 structures and spin density projected to atoms of FL, L-1, Ru-0, Ru-1, Ru-1-F, and Ru-1-Cl (PDF)

■ AUTHOR INFORMATION

Corresponding Authors

*E-mail: guohm@dlut.edu.cn (H.G.)
*E-mail: zhaojzh@dlut.edu.cn (J.Z.).

ORCID

Huimin Guo: 0000-0001-9283-7374
Jianzhang Zhao: 0000-0002-5405-6398
Bernhard Dick: 0000-0002-9693-5243

Author Contributions

H.M.G. designed this research after discussion with B.D. and J.Z.Z. and drafted the manuscript. H.M.G. and J.Z.Z. contributed materials and analysis tools. C.D. performed the theoretical calculations with the guidance of H.M.G. C.D. is responsible for the results presented. B.D. and J.Z.Z. commented the manuscript. The manuscript was revised through contributions of all authors. H.M.G. finalized the manuscript. All authors have given approval to the final version of the manuscript.

Notes

The authors declare no competing financial interest.

■ ACKNOWLEDGMENTS

This work was supported by National Natural Science Foundation of China (NSFC, Nos.: 21573034, 21771029, 11811530631, 21373036, and 21103015). B.D. thanks Dalian University of Technology for the Seasky Professorship. The supercomputer time was provided by National Supercomputing Center in Guangzhou, China, and the High Performance Computing Center at Dalian University of Technology.

■ REFERENCES

(1) Gueret, R.; Poulard, L.; Oshinowo, M.; Chauvin, J.; Dahmane, M.; Dupeyre, G.; Laine, P. P.; Fortage, J.; Collomb, M. N. Challenging the Ru(bpy)(3) (2+) Photosensitizer with a Triazatriangulenium Robust Organic Dye for Visible-Light-Driven Hydrogen Production in Water. *ACS Catal.* **2018**, *8* (5), 3792−3802.

(2) Parasram, M.; Gevorgyan, V. Visible light-induced transition metal-catalyzed transformations: beyond conventional photosensitizers. *Chem. Soc. Rev.* **2017**, *46* (20), 6227−6240.

(3) Zarkadoulas, A.; Koutsouri, E.; Kefalidi, C.; Mitsopoulou, C. A. Rhenium complexes in homogeneous hydrogen evolution. *Coord. Chem. Rev.* **2015**, *304*, 55−72.

(4) Stoll, T.; Castillo, C. E.; Kayanuma, M.; Sandroni, M.; Daniel, C.; Odobel, F.; Fortage, J.; Collomb, M. N. Photo-induced redox catalysis for proton reduction to hydrogen with homogeneous molecular systems using rhodium-based catalysts. *Coord. Chem. Rev.* **2015**, *304*, 20−37.

(5) Ashen-Garry, D.; Selke, M. Singlet Oxygen Generation by Cyclometalated Complexes and Applications. *Photochem. Photobiol.* **2014**, *90* (2), 257−274.

(6) Zhao, Q. A.; Li, F. Y.; Huang, C. H. Phosphorescent chemosensors based on heavy-metal complexes. *Chem. Soc. Rev.* **2010**, *39* (8), 3007−3030.

(7) Fernandez-Moreira, V.; Thorp-Greenwood, F. L.; Coogan, M. P. Application of d(6) transition metal complexes in fluorescence cell imaging. *Chem. Commun.* **2010**, *46* (2), 186−202.

(8) Baggaley, E.; Weinstein, J. A.; Williams, J. A. G. Lighting the way to see inside the live cell with luminescent transition metal complexes. *Coord. Chem. Rev.* **2012**, *256* (15−16), 1762−1785.

(9) Elmes, R. B. P.; Erby, M.; Bright, S. A.; Williams, D. C.; Gunnlaugsson, T. Photophysical and biological investigation of novel luminescent Ru(II)-polypyridyl-1,8-naphthalimide Troger's bases as cellular imaging agents. *Chem. Commun.* **2012**, *48* (20), 2588−2590.

(10) Lo, K. K. W.; Choi, A. W. T.; Law, W. H. T. Applications of luminescent inorganic and organometallic transition metal complexes as biomolecular and cellular probes. *Dalton Trans.* **2012**, *41* (20), 6021−6047.

(11) Gorman, A.; Killoran, J.; O'Shea, C.; Kenna, T.; Gallagher, W. M.; O'Shea, D. F. In vitro demonstration of the heavy-atom effect for photodynamic therapy. *J. Am. Chem. Soc.* **2004**, *126* (34), 10619−10631.

(12) McDonnell, S. O.; Hall, M. J.; Allen, L. T.; Byrne, A.; Gallagher, W. M.; O'Shea, D. F. Supramolecular photonic therapeutic agents. *J. Am. Chem. Soc.* **2005**, *127* (47), 16360−16361.

(13) Wu, W. T.; Shao, X. D.; Zhao, J. Z.; Wu, M. B. Controllable Photodynamic Therapy Implemented by Regulating Singlet Oxygen Efficiency. *Adv. Sci.* **2017**, *4* (7), 1700113.

(14) Ceroni, P. Energy Up-Conversion by Low-Power Excitation: New Applications of an Old Concept. *Chem. - Eur. J.* **2011**, *17* (35), 9560−9564.

(15) Monguzzi, A.; Tubino, R.; Hoseinkhani, S.; Campione, M.; Meinardi, F. Low power, non-coherent sensitized photon up-conversion: modelling and perspectives. *Phys. Chem. Chem. Phys.* **2012**, *14* (13), 4322−4332.

(16) Wing-Wah, Y. V.; Chung-Chin, C. E. Photochemistry and Photophysics of Coordination Compounds: Gold. In *Photochemistry and Photophysics of Coordination Compounds II*; Balzani, V., Campagna, S., Eds.; Springer: Berlin, 2007; pp 269−309.

(17) Flamigni, L.; Barbieri, A.; Sabatini, C.; Ventura, B.; Barigelletti, F. Photochemistry and Photophysics of Coordination Compounds: Iridium. In *Photochemistry and Photophysics of Coordination Compounds II*; Balzani, V., Campagna, S., Eds.; Springer: Berlin, 2007; pp 143−203.

(18) Williams, J. A. G. Photochemistry and Photophysics of Coordination Compounds: Platinum. In *Photochemistry and Photophysics of Coordination Compounds II*; Balzani, V.; Campagna, S., Eds.; Springer: Berlin, 2007; pp 205−268.

(19) Campagna, S.; Puntoriero, F.; Nastasi, F.; Bergamini, G.; Balzani, V. Photochemistry and Photophysics of Coordination Compounds: Ruthenium. In *Photochemistry and Photophysics of Coordination Compounds I*; Balzani, V., Campagna, S., Eds.; Springer: Berlin, 2007; pp 117−214.

(20) Kasha, M. Phosphoescence and the Role of the Triplet State in the Electronic Excitation of Complex Molecules. *Chem. Rev.* **1947**, *41* (2), 401−419.

(21) Zhao, J. Z.; Ji, S. M.; Guo, H. M. Triplet-triplet annihilation based upconversion: from triplet sensitizers and triplet acceptors to upconversion quantum yields. *RSC Adv.* **2011**, *1* (6), 937−950.

(22) Zhao, J. Z.; Ji, S. M.; Wu, W. H.; Wu, W. T.; Guo, H. M.; Sun, J. F.; Sun, H. Y.; Liu, Y. F.; Li, Q. T.; Huang, L. Transition metal complexes with strong absorption of visible light and long-lived triplet excited states: from molecular design to applications. *RSC Adv.* **2012**, *2* (5), 1712−1728.

(23) Zhao, J. Z.; Wu, W. H.; Sun, J. F.; Guo, S. Triplet photosensitizers: from molecular design to applications. *Chem. Soc. Rev.* **2013**, *42* (12), 5323−5351.

(24) Chou, P. T.; Chi, Y.; Chung, M. W.; Lin, C. C. Harvesting luminescence via harnessing the photophysical properties of transition metal complexes. *Coord. Chem. Rev.* **2011**, *255* (21−22), 2653−2665.

DOI: 10.1021/acs.inorgchem.9b00713
Inorg. Chem. 2019, 58, 8486−8493

(25) Whittemore, T. J.; White, T. A.; Turro, C. New Ligand Design Provides Delocalization and Promotes Strong Absorption throughout the Visible Region in a Ru(II) Complex. *J. Am. Chem. Soc.* **2018**, *140* (1), 229−234.
(26) Guo, H.; Zhu, L.; Dang, C.; Zhao, J.; Dick, B. Synthesis and photophysical properties of ruthenium(II) polyimine complexes decorated with flavin. *Phys. Chem. Chem. Phys.* **2018**, *20* (25), 17504−17516.
(27) Zhao, J. Z.; Xu, K. J.; Yang, W. B.; Wang, Z. J.; Zhong, F. F. The triplet excited state of Bodipy: formation, modulation and application. *Chem. Soc. Rev.* **2015**, *44* (24), 8904−8939.
(28) Jager, M.; Freitag, L.; Gonzalez, L. Using computational chemistry to design Ru photosensitizers with directional charge transfer. *Coord. Chem. Rev.* **2015**, *304*, 146−165.
(29) Zhang, X.; Jacquemin, D.; Peng, Q.; Shuai, Z. G.; Escudero, D. General Approach To Compute Phosphorescent OLED Efficiency. *J. Phys. Chem. C* **2018**, *122* (11), 6340−6347.
(30) Jacquemin, D. What is the Key for Accurate Absorption and Emission Calculations, Energy or Geometry? *J. Chem. Theory Comput.* **2018**, *14* (3), 1534−1543.
(31) Daniel, C. Photochemistry and photophysics of transition metal complexes: Quantum chemistry. *Coord. Chem. Rev.* **2015**, *282*−*283*, 19−32.
(32) Jacquemin, D.; Escudero, D. Thermal equilibration between excited states or solvent effects: unveiling the origins of anomalous emissions in heteroleptic Ru(II) complexes. *Phys. Chem. Chem. Phys.* **2018**, *20* (17), 11559−11563.
(33) Le Bahers, T.; Bremond, E.; Ciofini, I.; Adamo, C. The nature of vertical excited states of dyes containing metals for DSSC applications: insights from TD-DFT and density based indexes. *Phys. Chem. Chem. Phys.* **2014**, *16* (28), 14435−14444.
(34) Escudero, D.; Jacquemin, D. Computational insights into the photodeactivation dynamics of phosphors for OLEDs: a perspective. *Dalton Trans.* **2015**, *44* (18), 8346−8355.
(35) Niehaus, T. A.; Hofbeck, T.; Yersin, H. Charge-transfer excited states in phosphorescent organo-transition metal compounds: a difficult case for time dependent density functional theory? *RSC Adv.* **2015**, *5* (78), 63318−63329.
(36) Peng, Q.; Niu, Y. L.; Shi, Q. H.; Gao, X.; Shuai, Z. G. Correlation Function Formalism for Triplet Excited State Decay: Combined Spin-Orbit and Nonadiabatic Couplings. *J. Chem. Theory Comput.* **2013**, *9* (2), 1132−1143.
(37) Shuai, Z. G.; Peng, Q. Excited states structure and processes: Understanding organic light-emitting diodes at the molecular level. *Phys. Rep.* **2014**, *537* (4), 123−156.
(38) Shuai, Z. G.; Wang, D.; Peng, Q.; Geng, H. Computational Evaluation of Optoelectronic Properties for Organic/Carbon Materials. *Acc. Chem. Res.* **2014**, *47* (11), 3301−3309.
(39) Zhang, T.; Ma, H. L.; Niu, Y. L.; Li, W. Q.; Wang, D.; Peng, Q.; Shuai, Z. G.; Liang, W. Z. Spectroscopic Signature of the Aggregation-Induced Emission Phenomena Caused by Restricted Nonradiative Decay: A Theoretical Proposal. *J. Phys. Chem. C* **2015**, *119* (9), 5040−5047.
(40) Peng, Q.; Yi, Y. P.; Shuai, Z. G.; Shao, J. S. Toward quantitative prediction of molecular fluorescence quantum efficiency: Role of Duschinsky rotation. *J. Am. Chem. Soc.* **2007**, *129* (30), 9333−9339.
(41) Peng, Q.; Shi, Q. H.; Niu, Y. L.; Yi, Y. P.; Sun, S. R.; Li, W. Q.; Shuai, Z. G. Understanding the efficiency drooping of the deep blue organometallic phosphors: a computational study of radiative and non-radiative decay rates for triplets. *J. Mater. Chem. C* **2016**, *4* (28), 6829−6838.
(42) Yip, A. M. H.; Lo, K. K. W. Luminescent rhenium(I), ruthenium(II), and iridium(III) polypyridine complexes containing a poly(ethylene glycol) pendant or bioorthogonal reaction group as biological probes and photocytotoxic agents. *Coord. Chem. Rev.* **2018**, *361*, 138−163.
(43) Heinemann, F.; Karges, J.; Gasser, G. Critical Overview of the Use of Ru(II) Polypyridyl Complexes as Photosensitizers in One-Photon and Two-Photon Photodynamic Therapy. *Acc. Chem. Res.* **2017**, *50* (11), 2727−2736.
(44) Wright, I. A. Phosphorescent molecular metal complexes in heterojunction solar cells. *Polyhedron* **2018**, *140*, 84−98.
(45) Qu, F. R.; Park, S.; Martinez, K.; Gray, J. L.; Thowfeik, F. S.; Lundeen, J. A.; Kuhn, A. E.; Charboneau, D. J.; Gerlach, D. L.; Lockart, M. M.; Law, J. A.; Jernigan, K. L.; Chambers, N.; Zeller, M.; Piro, N. A.; Kassel, W. S.; Schmehl, R. H.; Paul, J. J.; Merino, E. J.; Kim, Y.; Papish, E. T. Ruthenium Complexes are pH-Activated Metallo Prodrugs (pHAMPs) with Light-Triggered Selective Toxicity Toward Cancer Cells. *Inorg. Chem.* **2017**, *56* (13), 7519−7532.
(46) Narayanam, J. M. R.; Stephenson, C. R. J. Visible light photoredox catalysis: applications in organic synthesis. *Chem. Soc. Rev.* **2011**, *40* (1), 102−113.
(47) Li, G.; Brady, M. D.; Meyer, G. J. Visible Light Driven Bromide Oxidation and Ligand Substitution Photochemistry of a Ru Diimine Complex. *J. Am. Chem. Soc.* **2018**, *140* (16), 5447−5456.
(48) Binning, R. C.; Curtiss, L. A. Compact Contracted Basis-Sets for 3rd-Row Atoms - GA-KR. *J. Comput. Chem.* **1990**, *11* (10), 1206−1216.
(49) Francl, M. M.; Pietro, W. J.; Hehre, W. J.; Binkley, J. S.; Gordon, M. S.; Defrees, D. J.; Pople, J. A. Self-Consistent Molecular-Orbital Methods 0.23. a Polarization-Type Basis Set for 2nd-Row Elements. *J. Chem. Phys.* **1982**, *77* (7), 3654−3665.
(50) Rassolov, V. A.; Ratner, M. A.; Pople, J. A.; Redfern, P. C.; Curtiss, L. A. 6-31G*basis set for third-row atoms. *J. Comput. Chem.* **2001**, *22* (9), 976−984.
(51) Hay, P. J.; Wadt, W. R. Abinitio Effective Core Potentials for Molecular Calculations - Potentials for the Transition-Metal Atoms Sc to Hg. *J. Chem. Phys.* **1985**, *82* (1), 270−283.
(52) Wadt, W. R.; Hay, P. J. Abinitio Effective Core Potentials for Molecular Calculations - Potentials for Main Group Elements NA TO BI. *J. Chem. Phys.* **1985**, *82* (1), 284−298.
(53) Miertus, S.; Scrocco, E.; Tomasi, J. Electrostatic Interaction of a Solute with a Continuum - a Direct Utilization of Abinitio Molecular Potentials for the Prevision of Solvent Effects. *Chem. Phys.* **1981**, *55* (1), 117−129.
(54) Cammi, R.; Mennucci, B. Linear response theory for the polarizable continuum model. *J. Chem. Phys.* **1999**, *110* (20), 9877−9886.
(55) Tomasi, J.; Mennucci, B.; Cammi, R. Quantum mechanical continuum solvation models. *Chem. Rev.* **2005**, *105* (8), 2999−3093.
(56) Becke, A. D. Density-Functional Thermochemistry 0.3. the Role of Exact Exchange. *J. Chem. Phys.* **1993**, *98* (7), 5648−5652.
(57) Lee, C. T.; Yang, W. T.; Parr, R. G. Development of the Colle-Salvetti Correlation-Energy Formula into a Functional of the Electron-Density. *Phys. Rev. B: Condens. Matter Mater. Phys.* **1988**, *37* (2), 785−789.
(58) Frisch, M. J.; Trucks, G. W.; Schlegel, H. B.; Scuseria, G. E.; Robb, M. A.; Cheeseman, J. R.; Scalmani, G.; Barone, V.; Petersson, G. A.; Nakatsuji, H.; Li, X.; Caricato, M.; Marenich, A. V.; Bloino, J.; Janesko, B. G.; Gomperts, R.; Mennucci, B.; Hratchian, H. P.; Ortiz, J. V.; Izmaylov, A. F.; Sonnenberg, J. L.; Williams-Yang, D.; Ding, F.; Lipparini, F.; Egidi, F.; Goings, J.; Peng, B.; Petrone, A.; Henderson, T.; Ranasinghe, D.; Zakrzewski, V. G.; Gao, J.; Rega, N.; Zheng, G.; Liang, W.; Hada, M.; Ehara, M.; Toyota, K.; Fukuda, R.; Hasegawa, J.; Ishida, M.; Nakajima, T.; Honda, Y.; Kitao, O.; Nakai, H.; Vreven, T.; Throssell, K.; Montgomery, J. A., Jr.; Peralta, J. E.; Ogliaro, F.; Bearpark, M. J.; Heyd, J. J.; Brothers, E. N.; Kudin, K. N.; Staroverov, V. N.; Keith, T. A.; Kobayashi, R.; Normand, J.; Raghavachari, K.; Rendell, A. P.; Burant, J. C.; Iyengar, S. S.; Tomasi, J.; Cossi, M.; Millam, J. M.; Klene, M.; Adamo, C.; Cammi, R.; Ochterski, J. W.; Martin, R. L.; Morokuma, K.; Farkas, O.; Foresman, J. B.; Fox, D. J. *Gaussian 09*, Revision D.01; Gaussian, Inc.: Wallingford, CT, 2016.
(59) Vahtras, O.; Agren, H.; Jorgensen, P.; Jensen, H. J. A.; Helgaker, T.; Olsen, J. Multiconfigurational Quadratic Response Functions for Singlet and Triplet Perturbations - the Phosphorescence Lifetime of Formaldehyde. *J. Chem. Phys.* **1992**, *97* (12), 9178−9187.

DOI: 10.1021/acs.inorgchem.9b00713
Inorg. Chem. 2019, 58, 8486−8493

(60) Hettema, H.; Jensen, H. J. A.; Jorgensen, P.; Olsen, J. Quadratic Response Functions for a Multiconfigurational Self-Consistent Field Wave-Function. *J. Chem. Phys.* **1992**, *97* (2), 1174−1190.
(61) Agren, H.; Vahtras, O.; Koch, H.; Jorgensen, P.; Helgaker, T. Direct Atomic Orbital Based Self-Consistent-Field Calculations of Nonlinear Molecular-Properties - Application to the Frequency-Dependent Hyperpolarizability of Para-Nitroaniline. *J. Chem. Phys.* **1993**, *98* (8), 6417−6423.
(62) Olsen, J.; Yeager, D. L.; Jorgensen, P. Triplet Excitation Properties in Large-Scale Multiconfiguration Linear Response Calculations. *J. Chem. Phys.* **1989**, *91* (1), 381−388.
(63) Jorgensen, P.; Jensen, H. J. A.; Olsen, J. Linear Response Calculations for Large-Scale Multiconfiguration Self-Consistent Field Wave-Functions. *J. Chem. Phys.* **1988**, *89* (6), 3654−3661.
(64) Aidas, K.; Angeli, C.; Bak, K. L.; Bakken, V.; Bast, R.; Boman, L.; Christiansen, O.; Cimiraglia, R.; Coriani, S.; Dahle, P.; Dalskov, E. K.; Ekstrom, U.; Enevoldsen, T.; Eriksen, J. J.; Ettenhuber, P.; Fernandez, B.; Ferrighi, L.; Fliegl, H.; Frediani, L.; Hald, K.; Halkier, A.; Hattig, C.; Heiberg, H.; Helgaker, T.; Hennum, A. C.; Hettema, H.; Hjertenaes, E.; Host, S.; Hoyvik, I. M.; Iozzi, M. F.; Jansik, B.; Jensen, H. J. A.; Jonsson, D.; Jorgensen, P.; Kauczor, J.; Kirpekar, S.; Kjaergaard, T.; Klopper, W.; Knecht, S.; Kobayashi, R.; Koch, H.; Kongsted, J.; Krapp, A.; Kristensen, K.; Ligabue, A.; Lutnaes, O. B.; Melo, J. I.; Mikkelsen, K. V.; Myhre, R. H.; Neiss, C.; Nielsen, C. B.; Norman, P.; Olsen, J.; Olsen, J. M. H.; Osted, A.; Packer, M. J.; Pawlowski, F.; Pedersen, T. B.; Provasi, P. F.; Reine, S.; Rinkevicius, Z.; Ruden, T. A.; Ruud, K.; Rybkin, V. V.; Salek, P.; Samson, C. C. M.; de Meras, A. S.; Saue, T.; Sauer, S. P. A.; Schimmelpfennig, B.; Sneskov, K.; Steindal, A. H.; Sylvester-Hvid, K. O.; Taylor, P. R.; Teale, A. M.; Tellgren, E. I.; Tew, D. P.; Thorvaldsen, A. J.; Thogersen, L.; Vahtras, O.; Watson, M. A.; Wilson, D. J. D.; Ziolkowski, M.; Agren, H. The Dalton quantum chemistry program system. *Wiley Interdiscip. Rev.-Comput. Mol. Sci.* **2014**, *4* (3), 269−284.
(65) Peng, Q.; Yi, Y. P.; Shuai, Z. G.; Shao, J. S. Excited state radiationless decay process with Duschinsky rotation effect: Formalism and implementation. *J. Chem. Phys.* **2007**, *126* (11), 114302.
(66) Niu, Y. L.; Peng, Q. A.; Deng, C. M.; Gao, X.; Shuai, Z. G. Theory of Excited State Decays and Optical Spectra: Application to Polyatomic Molecules. *J. Phys. Chem. A* **2010**, *114* (30), 7817−7831.
(67) Niu, Y.; Peng, Q.; Shuai, Z. Promoting-mode free formalism for excited state radiationless decay process with Duschinsky rotation effect. *Sci. China, Ser. B: Chem.* **2008**, *51* (12), 1153−1158.
(68) You, Y.; Park, S. Y. Phosphorescent iridium(III) complexes: toward high phosphorescence quantum efficiency through ligand control. *Dalton Trans.* **2009**, No. 8, 1267−1282.
(69) Fu, H. S.; Cheng, Y. M.; Chou, P. T.; Chi, Y. Feeling blue? Blue phosphors for OLEDs. *Mater. Today* **2011**, *14* (10), 472−479.
(70) Wagenknecht, P. S.; Ford, P. C. Metal centered ligand field excited states: Their roles in the design and performance of transition metal based photochemical molecular devices. *Coord. Chem. Rev.* **2011**, *255* (5−6), 591−616.
(71) Escudero, D. Quantitative prediction of photoluminescence quantum yields of phosphors from first principles. *Chem. Sci.* **2016**, *7* (2), 1262−1267.
(72) Minaev, B.; Agren, H. Theoretical DFT study of phosphorescence from porphyrins. *Chem. Phys.* **2005**, *315* (3), 215−239.
(73) Koseki, S.; Fedorov, D. G.; Schmidt, M. W.; Gordon, M. S. Spin-orbit splittings in the third-row transition elements: Comparison of effective nuclear charge and full Breit-Pauli calculations. *J. Phys. Chem. A* **2001**, *105* (35), 8262−8268.
(74) Koseki, S.; Schmidt, M. W.; Gordon, M. S. Effective nuclear charges for the first- through third-row transition metal elements in spin-orbit calculations. *J. Phys. Chem. A* **1998**, *102* (50), 10430−10435.

DOI: 10.1021/acs.inorgchem.9b00713
Inorg. Chem. 2019, 58, 8486−8493